International Journal of Solids and Structures 67–68 (2015) 84–92

Contents lists available at ScienceDirect

International Journal of Solids and Structures

journal homepage: www.elsevier.com/locate/ijsolstr

Is smaller always stiffer? On size effects in supposedly generalised continua

M.A. Wheel [a,*], J.C. Frame [b], P.E. Riches [b]

[a] Department of Mechanical and Aerospace Engineering, University of Strathclyde, Glasgow G1 1XJ, UK
[b] Department of Biomedical Engineering, University of Strathclyde, Glasgow G4 0NW, UK

ARTICLE INFO

Article history:
Received 7 November 2014
Received in revised form 17 February 2015
Available online 13 April 2015

Keywords:
Generalised continua
Couple stress
Micropolar
Cosserat
Micromorphic
Size effect
Cortical bone

ABSTRACT

Heterogeneous materials having constitutive behaviour described by more generalised continuum theories incorporating additional degrees of freedom such as couple stress, micropolar or micromorphic elasticity are expected to exhibit size effects in which there is an apparent increase in stiffness as the size scale reduces. Here we briefly demonstrate that for a simple heterogeneous material the size effect predicted when loaded in bending depends on the nature of the sample surface. Diverse size effects may thus be exhibited by the same material. We then show by detailed finite element analysis of a more representative material with regular heterogeneity that this diversity of size effects might actually be observed in practice thereby providing an explanation for the contradictory size effects that have sometimes been reported for real materials.

1. Introduction

Materials, when loaded, are usually assumed to deform in a manner described by classical or Cauchy elasticity theory. Central to this theory is the notion of size independence, when the deformation induced is proportional to the loading, implying that the stiffness of the material is constant, this stiffness will then be maintained at any size scale. The almost universal acceptance of this theory has arisen because many engineering materials have repeatedly demonstrated such size independent behaviour across those size scales of interest. However, certain materials are known to exhibit size dependent behaviour when loaded. Examples include fabricated materials such as foams (Lakes, 1983, 1986; Anderson and Lakes, 1994) with either stochastic or regular void distributions, aggregates such as concrete, biological tissues such as bone (Yang and Lakes, 1982; Choi et al., 1990) and naturally occurring minerals. A common feature of these materials is that the size scale of their microstructure is sufficient to be able to influence their macroscopic behaviour which can thus exhibit size dependency. Even those materials that are conventionally regarded as possessing size independent behaviour because they are essentially homogeneous at the macro scale can exhibit size dependency when the overall material scale is reduced to that of the underlying microstructure (Fleck et al., 1994).

More generalised continuum theories capable of forecasting size dependent behaviour do exist. Some of these are based upon the notion of incorporating higher derivatives of the deformation in the constitutive equations while others contain additional degrees of freedom. The latter class includes in ascending order of sophistication: couple stress, Cosserat or micropolar and micromorphic elasticity theories (Eringen, 1999). One common feature of all of these theories is that they incorporate additional constitutive parameters that must be identified either experimentally or possibly by numerical simulation of virtual materials. The experimental approach invariably involves testing material samples of different sizes in loading modes such as torsion or bending that induce a non uniform state of stress and thereby reveal any size dependency (Lakes, 1995). The additional constitutive parameters may then be derived from the observed size effect. The aforementioned theories all predict a size effect in which stiffness apparently increases as size is reduced. Such behaviour has been predicted in materials comprised of a lattice of periodically arranged connectors (Bažant and Christensen, 1972) and identified experimentally in polymeric foams (Lakes, 1983, 1986; Anderson and Lakes, 1994) and other materials comprised of a regular array of circular voids in a homogeneous two dimensional matrix (Beveridge et al., 2013; Waseem et al., 2013; McGregor and Wheel, 2014). However, in some materials, such as cortical bone,

* Corresponding author. Tel.: +44 141 548 3307; fax: +44 141 552 5105.
E-mail address: marcus.wheel@strath.ac.uk (M.A. Wheel).

http://dx.doi.org/10.1016/j.ijsolstr.2015.03.026
0020-7683/

size effects involving both increasing and decreasing stiffness with reducing size have been reported in the literature (Yang and Lakes, 1982; Choi et al., 1990). Such contradictory behaviour has been attributed to surface damage induced in the sample during manufacture which may result in increased sample compliance and thereby corrupt the observed size effect. The importance of careful sample preparation has been emphasised as a requirement if the effects of any such corruption are to be minimised (Anderson and Lakes, 1994). While sample preparation may in part be responsible an unanticipated size effect might also be attributed to the inherent influence that the material heterogeneity itself has on the surface behaviour. Insight into this influence might be gained by augmenting the generalised continuum theory of the bulk material with a surface elasticity model, as considered most recently in Gao and Mahmoud (2014) for example, where size effects in transversely loaded beams were shown to depend on the combined behaviour of bulk and surface. However, a disadvantage in this approach is that the incorporation of the surface elasticity model introduces additional constitutive parameters that must be identified.

In this paper we present a straightforward analysis demonstrating that a rich variety of size effects might be expected in beam samples made of a simple heterogeneous material comprised of just two constituents of differing moduli layered alternately. Laminated materials of this type have previously been shown to demonstrate behaviour consistent with the predictions of Cosserat elasticity that includes the dispersion of propagating elastic waves when loaded dynamically (Herrmann and Achenbach, 1968) and also a dependence of stiffness on size when loaded statically (Forest and Sab, 1998). We then show by detailed finite element analysis that some of these size effects are actually exhibited in samples of a material with regular, periodic heterogeneity whose behaviour has previously been shown to be consistent with Cosserat elasticity theory. Finally, we compare the size effects predicted for the laminate material with those reported elsewhere in the literature for both virtual and real materials.

The key outcome of this paper is that we unambiguously identify the pertinent microstructural characteristics that affect the nature of experimentally, or virtually, observed size effects in heterogeneous media. It is also argued that in certain circumstances, bulk constitutive behaviour may be inferred even if the observed behaviour does not align with a generalised continuum theory.

2. A laminated beam model of a generalised continuum

Consider a slender beam composed of alternating layers or plies of two different materials of Young's moduli E_1 and E_2 respectively. All layers of the first material are all of thickness t_1 while all internal plies of the second material have thickness t_2. The upper and lower surface layers of the composite beam always consist of the second material and each has a thickness of rt_2 where $0 < r < 1$. If n is the number of plies of the first material then there will be $n-1$ internal layers of the second material. The total number of layers across an entire section of beam will therefore be $2n + 1$. When n is odd then the central layer of the beam will consist of the first material while in the case when n is even the central ply will be comprised of the second material. Both cases are illustrated in Fig. 1. In each case the beam section is symmetric about the neutral axis. The laminated material considered here thus bears some resemblance to one comprised of multiple layers of a simple biphasic constituent that was previously shown to exhibit size effects (Dai and Zhang, 2008) though these were not interpreted in the context of generalised continua. According to Bernoulli Euler beam theory the flexural rigidity, D, of the composite beam section can be obtained by deriving the products of the moduli and second moments of area about the section neutral axis of the individual plies and then summing these products. Thus in the case where n is odd this summation can be represented thus:-

$$D = 2\int_0^{t_1/2} E_1 by^2 dy + \sum_{i=1}^{(n-1)/2} 2\int_{(i-1/2)t_1+it_2}^{(i+1/2)t_1+it_2} E_1 by^2 dy + \sum_{i=1}^{(n-1)/2} 2\int_{(i-1/2)t_1+(i-1)t_2}^{(i-1/2)t_1+it_2} E_2 by^2 dy + 2\int_{(n/2)t_1+[(n-1)/2]t_2}^{(n/2)t_1+[(n-1+2r)/2]t_2} E_2 by^2 dy$$

while when n is even the summation is:-

$$D = 2\int_0^{t_2/2} E_2 by^2 dy + \sum_{i=1}^{n/2} 2\int_{(i-1/2)t_1+it_2}^{(i+1/2)t_1+it_2} E_1 by^2 dy + \sum_{i=1}^{n/2-1} 2\int_{it_1+(i-1/2)t_2}^{it_1+(i+1/2)t_2} E_2 by^2 dy + 2\int_{(n/2)t_1+[(n-1)/2]t_2}^{(n/2))t_1+[(n-1+2r)/2]t_2} E_2 by^2 dy$$

where b is the breadth of the beam and y the distance from the neutral axis. The first integral in each case accounts for the central layer of material while the summation terms are associated with intermediate layers of each material and the final integrals account for the surface layer comprised of the second material. Interestingly, when each of these summations is evaluated the following single expression for the flexural rigidity:-

$$D = \frac{1}{12}E_1 bt_1 n\left[n^2t_1^2 + 2(n^2-1)t_1t_2 + (n^2-1)t_2^2\right] + \frac{1}{12}E_2 bt_2\left\{\begin{array}{l}\left[6n^2r + n(n-1)(n-2)\right]t_1^2 + \left[12nr^2 + 12n(n-1)r + 2n(n-1)(n-2)\right]t_1t_2 + \\ \left[8r^3 + 12(n-1)r^2 + 6(n-1)^2r + (n-1)^3\right]t_2^2\end{array}\right\}$$

that applies in both cases is obtained. After expanding and collecting similar terms this expression for D can be represented thus:-

$$\begin{aligned} D = {} & \frac{E_1 bnt_1}{12}\left\{[nt_1 + (n-1+2r)t_2]^2 - 2t_2[t_1 + t_2 + 2r^2t_2 - nt_1 - nt_2 - 2rt_2 + 2nrt_1 + 2nrt_2]\right\} \\ & + \frac{E_2 b(n-1+2r)t_2}{12}\left\{[nt_1 + (n-1+2r)t_2]^2 + 2t_1[t_1 + t_2 + 2r^2t_2 - nt_1 - nt_2 - 2rt_2 + 2nrt_1 + 2nrt_2]\right\} \end{aligned} \quad (3)$$

The depth, d, of the beam is:-

$$d = nt_1 + (n-1+2r)t_2 \quad (4)$$

and if the length to depth aspect ratio of the beam is a then the length, L, of the beam is given by

$$L = a[nt_1 + (n-1+2r)t_2] \quad (5)$$

The stiffness, K, of the beam when loaded in three point bending is:-

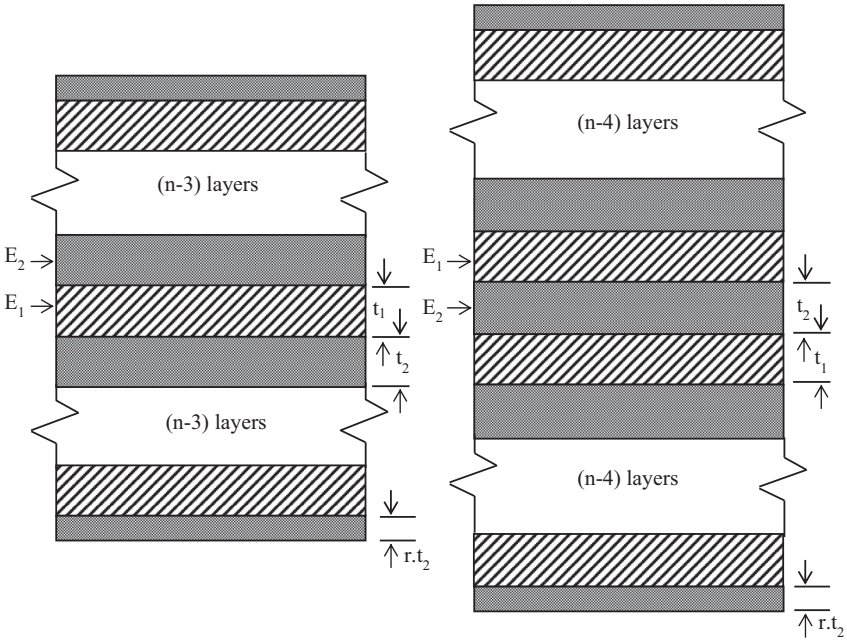

Fig. 1. Laminated beam model of heterogeneous material.

$$K = \frac{4E_1 bnt_1}{a^3[nt_1 + (n-1+2r)t_2]^3}\left\{[nt_1 + (n-1+2r)t_2]^2 - 2t_2\left[t_1 + t_2 + 2r^2t_2 - nt_1 - nt_2 - 2rt_2 + 2nrt_1 + 2nrt_2\right]\right\} + \frac{4E_2 b(n-1+2r)t_2}{a^3[nt_1 + (n-1+2r)t_2]^3}\left\{[nt_1 + (n-1+2r)t_2]^2 + 2t_1\left[t_1 + t_2 + 2r^2t_2 - nt_1 - nt_2 - 2rt_2 + 2nrt_1 + 2nrt_2\right]\right\} \quad (6)$$

which can be rearranged thus:-

$$K = \frac{4b[E_1 nt_1 + E_2(n-1+2r)t_2]}{a^3[nt_1 + (n-1+2r)t_2]^3}\left\{[nt_1 + (n-1+2r)t_2]^2\right\} + \frac{4b[E_2(n-1+2r)t_1t_2 - E_1nt_1t_2]}{a^3[nt_1 + (n-1+2r)t_2]^3}\left\{2\left[t_1 + t_2 + 2r^2t_2 - nt_1 - nt_2 - 2rt_2 + 2nrt_1 + 2nrt_2\right]\right\} \quad (7)$$

The stiffness of the beam when loaded in other bending configurations could be derived similarly, our interest in three point bending in particular is motivated by its simplicity which frequently renders it the loading mode of choice in practice.

By the rule of mixtures the average modulus of the beam section, E^*, is:-

$$E^* = \frac{E_1 nt_1 + E_2(n-1+2r)t_2}{nt_1 + (n-1+2r)t_2} \quad (8)$$

The first term in (7) can thus be simplified to leave the expression for the stiffness of the beam as:-

$$K = \frac{4E^* b}{a^3} + \frac{4b[E_2(n-1+2r)t_1t_2 - E_1nt_1t_2]}{a^3[nt_1 + (n-1+2r)t_2]^3}\left\{2\left[t_1 + t_2 + 2r^2t_2 - nt_1 - nt_2 - 2rt_2 + 2nrt_1 + 2nrt_2\right]\right\} \quad (9)$$

The first term in (9) is simply the stiffness of a slender homogeneous beam of modulus E^* loaded in three point bending while the second term quantifies the size effect associated with the heterogeneous nature of the laminated beam. Eq. (9) thus bears some similarity to the expression for the stiffness of a slender micropolar beam:-

$$K = 4E^* b\left(\frac{d}{L}\right)^3\left[1 + \left(\frac{l_c}{d}\right)^2\right] \quad (10)$$

which was derived by assuming that a linear variation in bending stress and a uniform state of couple stress acts on every cross section of the beam (Beveridge et al., 2013) and that any deformations in the transverse direction across the breadth of the beam can be ignored. Thus Eq. (10) represents a simplification of the more general solution for the deformation quoted in earlier literature (Lakes, 1995). The characteristic length, l_c, is a constitutive parameter that quantifies the length scale associated with the couple stresses. According to Eq. (10) the characteristic length can be identified from any size dependent stiffening effect that may be observed. The validity of Eq. (10) was confirmed by experimental testing and detailed finite element analysis of slender beam samples of a heterogeneous material comprised of periodically distributed circular voids within a homogeneous matrix (Beveridge et al., 2013). The breadth, b, was common to all samples. In accordance with Eq. (10) beam stiffness was found to increase linearly with the reciprocal of beam depth squared, $1/d^2$, for samples of the same aspect ratio. Analogous behaviour was observed in similar slender ring samples loaded diametrically [Waseem et al., 2013].

The key difference between Eqs. (9) and (10) is that in the latter case the predicted size effect will always be positive; smaller samples will be stiffer than their larger counterparts whereas in the former case the size effect may be more elaborate since the second term depends on the relative magnitudes of the ply moduli, E_1 and E_2, their thicknesses, t_1 and t_2, and the thickness of the surface layers as quantified by r.

Figs. 2–6 show how the predicted stiffness varies with sample size for a variety of combinations of material moduli, internal ply and surface layer thicknesses. In all of these figures the reciprocal of depth squared, $1/d^2$, is used to quantify the sample size and thereby facilitate a direct comparison of any predicted size effect with that forecast by Eq. (10). In each of these figures the stiffness

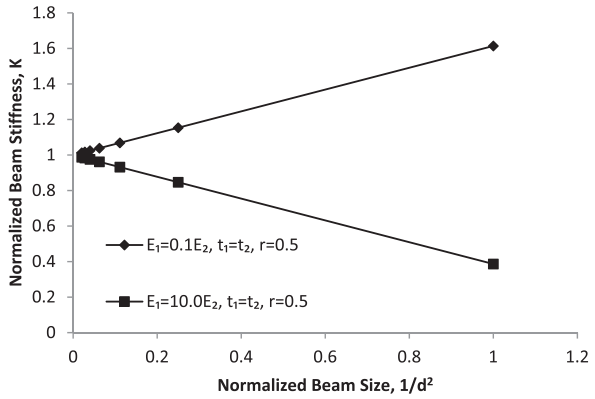

Fig. 2. Variation in stiffness with beam size for cases where $E_1 = 0.1E_2$, $t_1 = t_2$, $r = 0.5$ and $E_1 = 10.0E_2$, $t_1 = t_2$, $r = 0.5$.

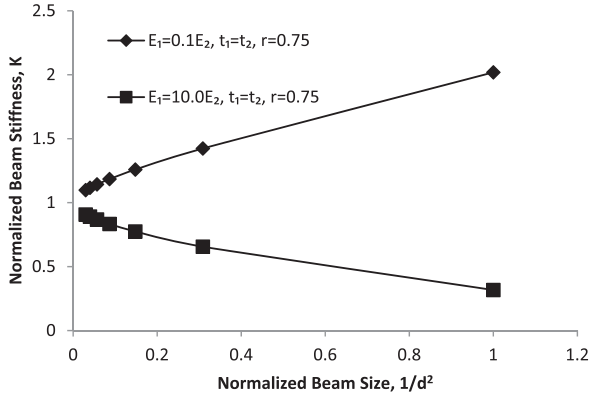

Fig. 3. Variation in stiffness with beam size for cases where $E_1 = 0.1E_2$, $t_1 = t_2$, $r = 0.75$ and $E_1 = 10.0E_2$, $t_1 = t_2$, $r = 0.75$.

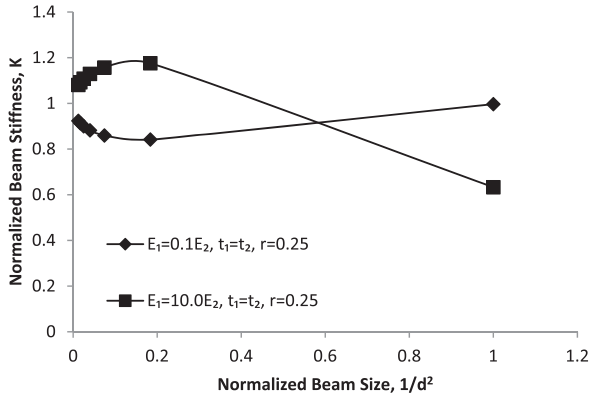

Fig. 4. Variation in stiffness with beam size for cases where $E_1 = 0.1E_2$, $t_1 = t_2$, $r = 0.25$ and $E_1 = 10.0E_2$, $t_1 = t_2$, $r = 0.25$.

has been normalised with respect to the leading term in Eq. (9), this being the stiffness of a beam on modulus, $E*$, that exhibits no size effect. This is equivalent to the stiffness of a beam of almost infinite depth, that is, a beam for which n is very large and the second term in Eq. (9) tends to zero. The size measure, $1/d^2$, has been normalised with respect to this measure for the thinnest possible beam, this being $1/(t_1 + 2rt_2)^2$. In addition, the stiffness variations shown in these figures assume a common sample breadth, b, of unity and aspect ratio, a, of 10. In Fig. 2 the internal layers of each material are assumed to be the same thickness while the thickness of the surface layers is set to half that of their internal counterparts

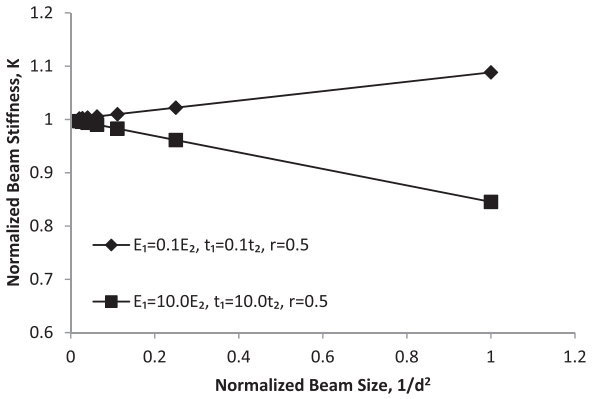

Fig. 5. Variation in stiffness with beam size for cases where $E_1 = 0.1E_2$, $t_1 = 0.1t_2$, $r = 0.5$ and $E_1 = 10.0E_2$, $t_1 = 10t_2$, $r = 0.5$.

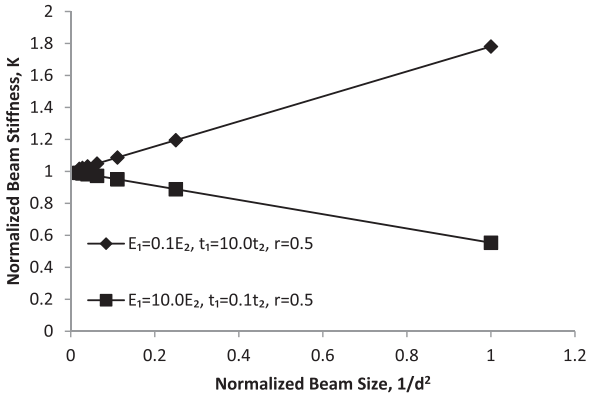

Fig. 6. Variation in stiffness with beam size for cases where $E_1 = 0.1E_2$, $t_1 = 10.0t_2$, $r = 0.5$ and $E_1 = 10.0E_2$, $t_1 = 0.1t_2$, $r = 0.5$.

by specifying $r = 0.5$. However, one of the materials is ten times stiffer than the other. When the material constituting the surface layers is the stiffer of the two a positive size effect is predicted, stiffness increases as size reduces, whereas when the surface is formed from the more compliant material a contrasting, negative size effect is seen. Furthermore, the positive size effect is apparently linear, as anticipated by Eq. (10), while the negative effect behaves similarly. Interestingly, although these size effects are opposite in character they seemingly have the same magnitude.

In Figs. 3 and 4 the material moduli and internal ply thicknesses are maintained but the thickness of the surface layers is varied by altering r. Fig. 3 depicts the size effects when $r = 0.75$. Evidently there is some similarity to the size effects shown in Fig. 2; when the surface layers are formed from the stiffer material the effect is positive but if the surfaces are comprised of the more compliant material the opposite effect is once again seen. However, there is a distinct difference in that the stiffness is now seen to vary nonlinearly with the sample size measure in both cases whereas previously each variation was linear. This nonlinearity in the size effect begins to appear as r is increased above 0.5 and is maintained up to $r = 1.0$. Fig. 4 shows that for $r = 0.25$ the size effects are noticeably different from those seen in Figs. 2 and 3. When the stiffer material forms the surfaces the size effect is negative at larger sample sizes but then changes to become positive as sample size reduces. The size effect exhibits the opposite behaviour when the surfaces are formed of the more compliant material. The inversion seen in both of these size effects appears progressively as r begins to reduce below 0.5. It becomes more pronounced as r is reduced further but then diminish and eventually begin to

disappear again as r approaches zero at which point the two effects then resemble those seen when $r = 1.0$ as might be expected.

Figs. 5 and 6 show the effect of varying the ratio of the ply thicknesses when their moduli are maintained at the same ratio and the thickness of the surfaces is half that of the equivalent internal layers. In Fig. 5 the stiff layers are 10 times thicker than the compliant plies. The size effects resemble those in Fig. 2; stiff surfaces yield a positive effect while compliant surfaces produce a negative effect and these are linear in both cases. However, the size effects are no longer equal in magnitude, the positive effect is smaller than the negative one. In Fig. 6 the situation is reversed, the thickness of stiff layers is 10 times less than that of the compliant plies. The magnitude of the positive size effect is now greater than the negative one as shown. Fig. 7 depicts how the magnitudes of both positive and negative size effects change as the volume fraction of compliant material, quantified by the ratio of the compliant layer thickness to the combined thickness of two adjacent layers, varies. When the volume fraction of compliant material is very low then both size effects are negligible since the beam samples are predominantly comprised of the stiffer material. As the volume fraction increases so does the magnitude of each size effect. At 50% volume fraction both size effects are of the same magnitude as already seen in Fig. 2. Beyond this they each continue to increase up to a maximum which occurs at around 66% and 83% for the negative and positive effects respectively. Beyond this the size effects diminish as the samples are now largely comprised of compliant material.

3. Size effects in a two dimensional medium with periodic heterogeneity

A two dimensional material with regular or periodic heterogeneity that has been investigated previously (Beveridge et al., 2013) in the context of generalised continua, specifically micropolar elasticity theory, is illustrated in Fig. 8. The heterogeneity results from introducing a regular array of circular voids into an otherwise classically elastic matrix material as illustrated. The geometry of the heterogeneity is fully defined by the void radius, V_R, and the separation of the void centres, S_x and S_y, in the indicated x and y directions respectively. The void centres lie on a triangular grid and when $S_y = \sqrt{3}S_x/2$ results of detailed of finite element analysis incorporating a sufficiently large number of voids indicate that the material exhibits approximate planar isotropy and is therefore transversely isotropic. The behaviour of the matrix material is described by its Young's modulus and Poisson's ratio in accordance with the assumption that it behaves in a classically elastic manner.

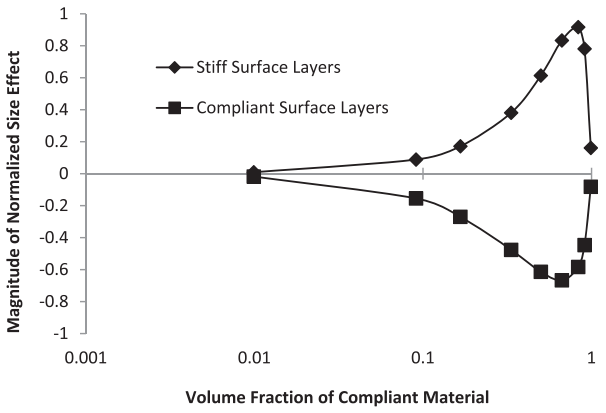

Fig. 7. Variation in the magnitudes of positive and negative size effects as a function of compliant material volume fraction.

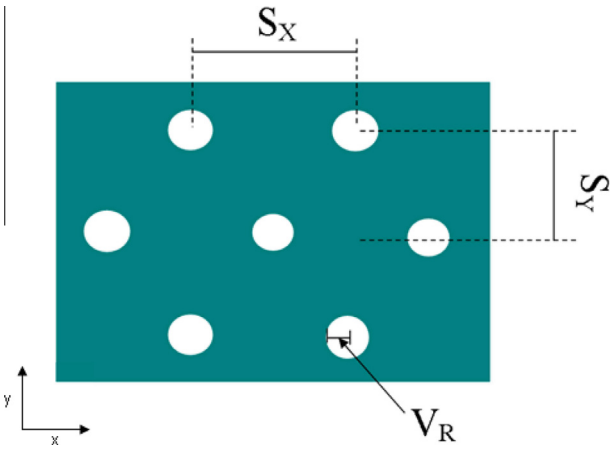

Fig. 8. Two dimensional material with regular, periodic heterogeneity investigated previously within the context of micropolar elasticity theory.

Finite element analysis of slender beam samples of different depths but the same aspect ratio revealed that this material exhibited a size dependent stiffening consistent with Eq. (10) (Beveridge et al., 2013). In generating the mesh required for each analysis a structured array of quadratic quadrilateral elements illustrated in Fig. 9 was used to represent the perforated rectangular region of matrix material surrounding each void so that the details of the heterogeneity were explicitly represented. As a consequence of generating the mesh representing each sample in this way the upper and lower surfaces were each implicitly located midway between adjacent, axially aligned rows of voids and hence none

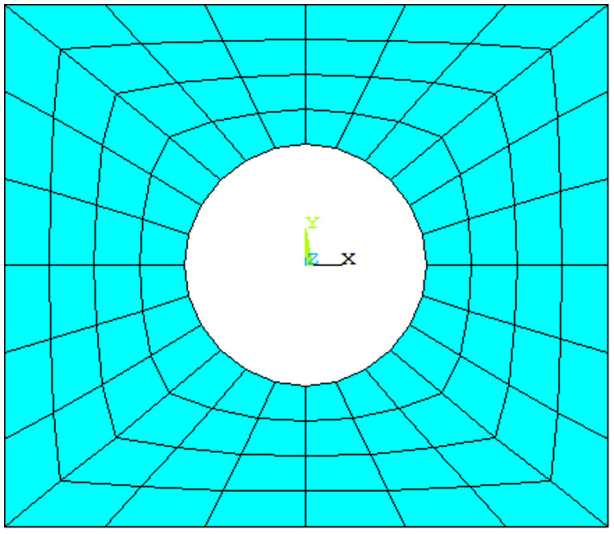

Fig. 9. Structured mesh of quadratic quadrilateral finite elements used to represent rectangular region around a particular void within two dimensional heterogeneous material.

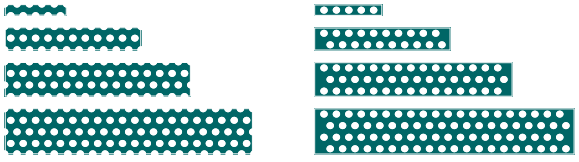

Fig. 10. Representation of beam samples of increasing size generated by finite element meshes shown in Figs. 9 (right) and 11 (left).

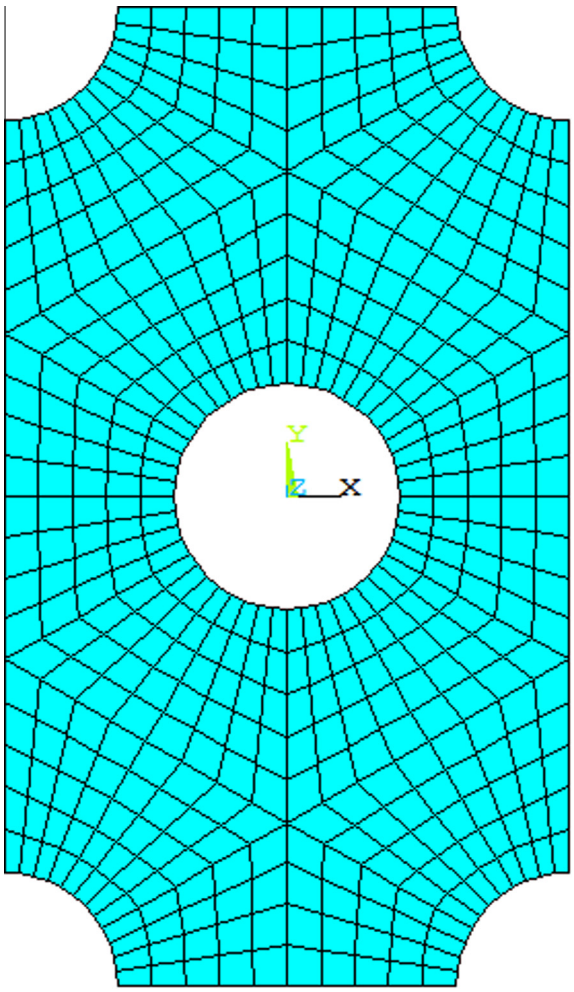

Fig. 11. Alternative mesh of quadratic quadrilateral finite elements used to represent region between neighbouring voids within two dimensional heterogeneous material.

of the voids intersected these surfaces as illustrated in Fig. 10. However, locating the surfaces in this manner constitutes only one particular means of identifying the beam samples from within a larger piece of the material. The samples could reasonably be identified in alternative ways in which the surfaces intersect the voids. Another means of generating the finite element mesh of the matrix material, shown in Fig. 11, has therefore been employed here to investigate one alternative. Although a structured mesh is once again exploited in representing the matrix material between a specific void and its neighbours it does enable an alternative in which the sample surfaces periodically bisect all voids in a given row, as also shown in Fig. 10, to be readily investigated. This means of mesh generation was therefore used to analyse beams of increasing depth, this being determined by the number of rows of voids with the smallest beam containing just a single row and the largest four rows as shown in Fig. 10. The void separations, S_x and S_y, were prescribed at 1.0 mm and 0.866 mm respectively while the length to depth aspect ratio was set at 10.4:1 thus fixing the overall dimensions of each beam. The Young's modulus and Poisson's ratio of the matrix material were set to 20 GPa and 0.3 respectively and plane stress behaviour assumed. Constraints and loading representative of three point bending were then applied but since geometry and loading are both symmetric suitable boundary conditions were imposed at the central loading plane to facilitate analysis of only one half of each beam thereby reducing computational effort.

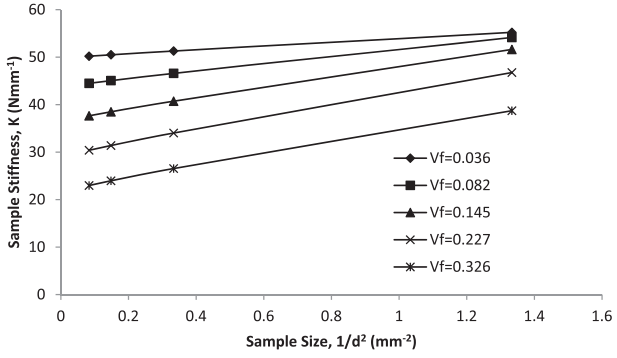

Fig. 12. Stiffness against the reciprocal of depth squared for beams with smooth surfaces at a 10.4:1 length to depth aspect ratio for various void volume fractions, *Vf*.

Fig. 12 shows the predicted variations in beam stiffness with size for different void volume fractions, *Vf*, when the voids and surfaces do not intersect. Evidently, at any given void size, the stiffness variation is approximately linear. According to Eq. (10) the modulus of each material can thus be derived from the intercept of the corresponding variation while the characteristic length can be obtained from the slope. Values of these two constitutive parameters are listed in table 1 as a function of void radius and volume fraction. Data derived from the stiffness variations determined when the sample aspect ratio is increased to 20.8:1 are also listed. It can be seen from the data presented in this table that as the void radius increases the modulus reduces as might be expected since the amount of matrix material capable of supporting the applied loading is decreasing. However, the characteristic length increases as the void radius is increased. Moreover, the differences in the values of this constitutive parameter obtained at aspect ratios of 10.4:1 and 20.8:1 are slight implying that although Eq. (10) assumes slender beam behaviour the lower, 10.4:1, aspect ratio beams are sufficiently slender enough to satisfy this assumption and thereby provide very reasonable estimates of the characteristic length. Fig. 13, which depicts the relationship between void radius and characteristic length for the higher, 20.8:1, aspect ratio beams, clearly shows that this is linear thus corroborating theoretical predictions for both Cosserat materials (Bigoni and Drugan, 2007) and generalised continua of the second order Mindlin type (Bacca et al., 2013a, 2013b).

Variations in beam stiffness with size for the same set of void radii when the surfaces now bisect the voids are shown in figure 14. Obviously these variations no longer concur with Eq. (10), they each now show a decrease in stiffness with reducing size. Nonetheless each variation is linear which does accord with Eq. (9) for the case where $r = 0.5$. In addition, the intercept of a given

Table 1
Comparison of the characteristic lengths for different void radii at 10.4:1 and 20.8:1 length to depth aspect ratios.

Void Diameter, V_d (mm)	Void Fraction *Vf*	Normalised void radius V_R/S_Y	Young's Modulus (GPa)		Characteristic length (mm)	
			10.4:1 aspect ratio	20.8:1 aspect ratio	10.4:1 aspect ratio	20.8:1 aspect ratio
0.2	0.036	0.12	17.47	17.87	0.28	0.28
0.3	0.082	0.17	15.37	15.71	0.42	0.43
0.4	0.145	0.23	12.90	13.16	0.55	0.57
0.5	0.227	0.29	10.31	10.50	0.66	0.70
0.6	0.326	0.35	7.74	7.83	0.75	0.82

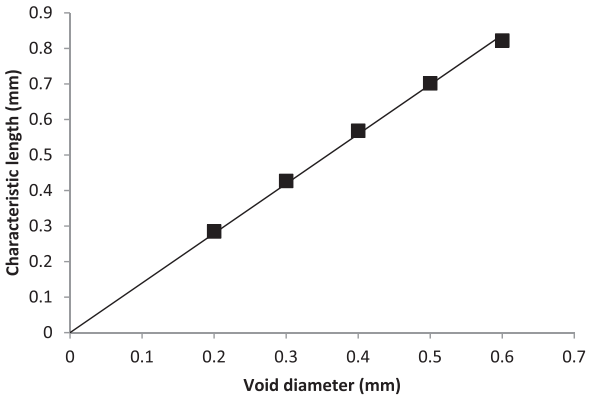

Fig. 13. Variation in micropolar characteristic length with void diameter for 20.8:1 aspect ratio beams.

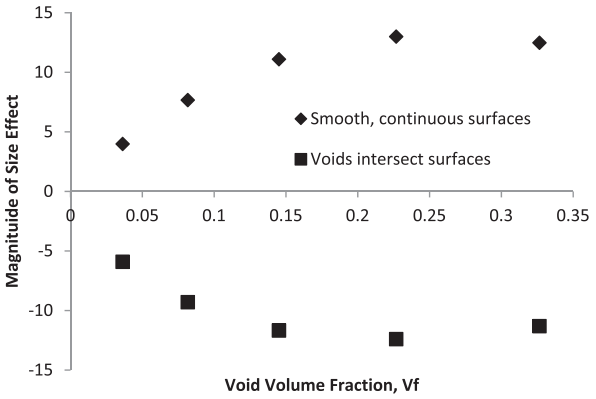

Fig. 15. The magnitude of the size effects as a function of void volume fraction *Vf* for beams with both smooth and intersected surfaces and a 20.8:1 length to depth aspect ratio.

negative size effect seen in this figure is the same as that of the positive effect for the corresponding void radius shown in Fig. 12. This reflects the convergence of both effects at large beam depths seen in Fig. 2. The magnitudes of the positive size effects seen in Fig. 12 along with those of their negative counterparts observed in Fig. 14 have been determined for each void radius considered and are shown as a function of the void volume fraction in Fig. 15 with the volume fraction having been straightforwardly derived from the void radii and separations beforehand. As Fig. 15 demonstrates the variation in the magnitude of the negative effect broadly reflects that of the positive effect and, moreover, they both emulate the variations shown in Fig. 7; at low volume fractions each size effect is small but increases with volume fraction up to a maximum beyond which they begin to reduce again.

4. Size effects predicted in a two dimensional stochastic foam and observed in cortical bone

Forecasts of the size effect expected in two dimensional foams were made previously (Tekoglu and Onck, 2008) by representing the stochastic cellular microstructure as random Voronoi tessellations with individual sections of cell wall being represented by Timoshenko beam finite elements. While all internal cells within an elongated rectangular region were represented by closed polygons those cells intersecting the boundary remained open, no elements were located coincident to the boundary to close them. Fig. 16 shows the details of the beam finite element mesh in the vicinity of the rectangular region boundary. Rupturing of those cells adjacent to the surface is clearly seen in the inset detail. The discrete representations were loaded in simple shear, uniaxial compression and pure bending of the major axis. Multiple analyses were conducted for each of these loading modes using a different randomly generated finite element mesh on each occasion in order to capture the behaviour of the stochastic microstructure. For each analysis a constant rotation was imposed on the mesh at the ends of the rectangular region by applying linearly varying displacements. The resulting moment was then determined from the computed reaction forces. Bending stiffness could thus be calculated from the ratio of resulting moment to imposed rotation.

The bending stiffness of the material was found to change with beam depth, this being varied by altering the lesser dimension of the representative rectangular region. Results were presented graphically with the stiffness, normalised with respect to the bending stiffness anticipated by classical beam theory, being plotted against beam depth, this being normalised with respect to the average cell size. At small depths forecast stiffness was less than classically anticipated but was found to rise and asymptotically approach the classical result as depth increased. In Fig. 17 the size effect seen in Fig. 2 for the laminated beam with compliant surface layers is once again shown but now the normalised stiffness is plotted as a function of the beam depth where this is normalised with respect to the average depth of the stiff and compliant layers. When presented in this manner the size effect observed in the laminated beams closely resembles that forecast for the two dimensional foam material.

Size effects have also been observed previously (Yang and Lakes, 1982; Choi et al., 1990) in experiments where human cortical bone samples were loaded in bending. The results of these investigations are contradictory with the earlier work reporting a positive size effect while the later reported an opposite, negative

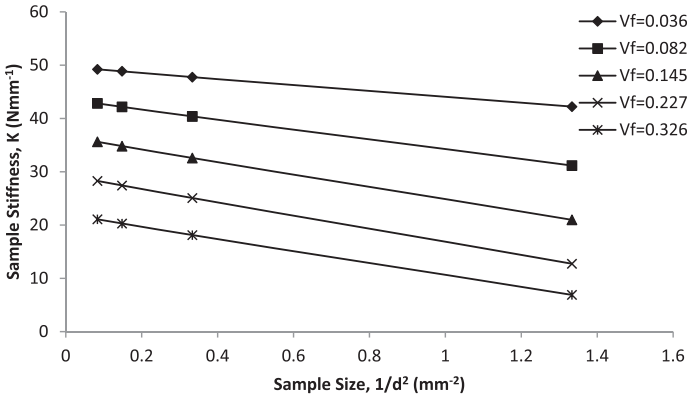

Fig. 14. Stiffness against the reciprocal of depth squared for beams with intersected surfaces at a 10.4:1 length to depth aspect ratio for various void volume fractions, *Vf*.

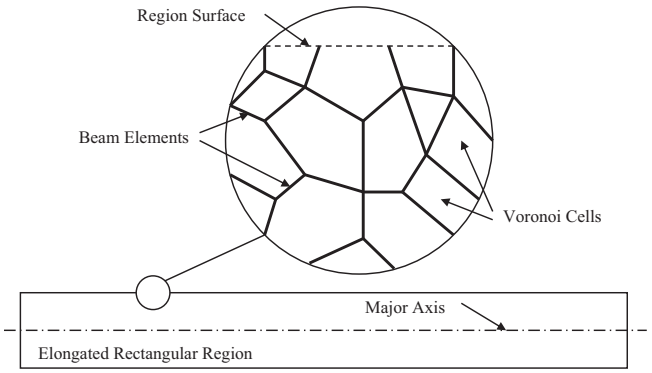

Fig. 16. Surface details of two dimensional foam material studied previously (Tekoglu and Onck, 2008).

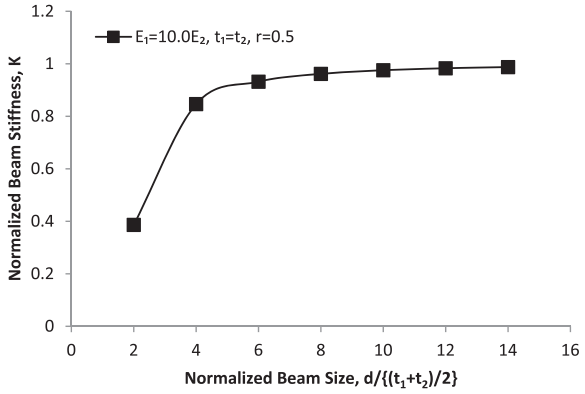

Fig. 17. Variation in stiffness with beam depth in the case where $E_1 = 10.0E_2$, $t_1 = t_2$, $r = 0.5$.

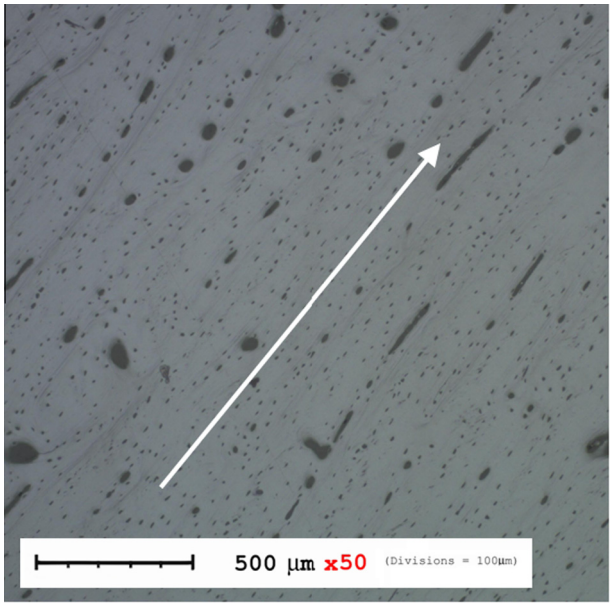

Fig. 18. Section of cortical bone illustrating partial exposure of vascular channels at section surface (arrow indicates channel principal orientation).

effect. In the earlier work beam specimens with depths ranging from 5.2 mm down to 1.4 mm were tested while in the later investigation samples were divided into two categories, those with a depth of greater than 0.5 mm and those with a depth of less than

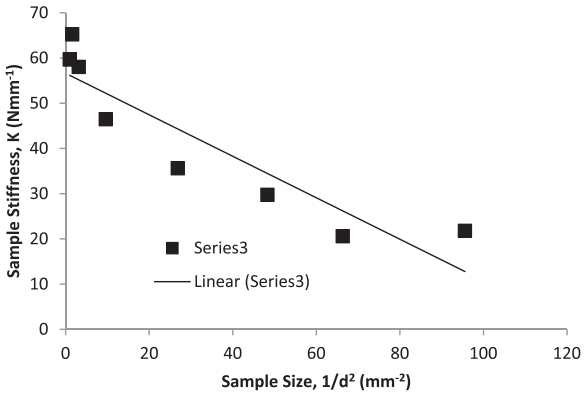

Fig. 19. Variation in stiffness with size for human cortical bone samples of unit width (based on data reported by Choi e0074 al. (1990)).

0.5 mm. The most significant size effect was observed in samples in the latter category. The latter investigators questioned the validity of the earlier work and suggested that the true nature of the size effect was only revealed by testing the smaller sized samples. They then suggested a qualitative explanation of the size effect based on the enhanced compliance of the material adjacent to the sample surfaces resulting from the interaction of the major microstructural feature, the nutrient transporting vascular channel or Haversian canal system, with the sample surfaces themselves. Fig. 18 shows an optical microscope image of a section of cortical bone with the section surface lying parallel to the channel orientation. The partial exposure of the tubular channels at the surface is clearly visible thereby supporting the suggested explanation for the increased compliance of the adjacent material. However, despite the suggested explanation they interpreted the measured size effect quantitatively as a reduction in the apparent modulus of the material, this being determined from the measured stiffness using classical elasticity based beam theory. No attempt was made to explain this reduction in apparent modulus in the context of generalised continuum theories.

While the investigators did not explicitly report the experimentally measured stiffness of each sample they tested they did provide full details of sample size and geometry when reporting their results for the apparent material modulus. It has thus possible for us to calculate the stiffness of each sample from their published data using beam theory. Since each of their samples had an approximately square cross section we have then normalised the calculated sample stiffness data with respect to sample breadth to facilitate comparison with sample sets of common breadth. Fig. 19 shows the variation in this normalised stiffness with sample size where, as earlier, this is quantified by the reciprocal of beam depth squared. When presented in this format the data shown in Fig. 19 reflect those shown in Figs. 2 and 3 for the cases where $E_2 < E_1$, that is, the surface layers are comprised of the more compliant of the two constituent materials.

5. Discussion and conclusions

When loaded in bending the simple two phase laminate material considered in this paper exhibits an intriguing variety of size effects which, under certain circumstances identified explicitly here, are compatible with the predictions of generalised continuum theories in that stiffness appears to increase as overall size reduces. Such behaviour has thus been categorised as a positive effect. However, in other situations that have also been established the predicted size effect is entirely different in character, the material apparently becomes more compliant as size is decreased, behaviour which has therefore been classified as a negative effect. The circumstances determining the nature of the size effect appear to

be governed entirely by the surface state of the material. A negative size effect may be expected when the surface layer is both greater than a certain minimum thickness and more compliant than the bulk material. Any reduction in the thickness of the compliant surface layer below the minimum may however result in a more elaborate size effect the nature of which is also strongly size dependent.

Negative size effects have been reported in both real and computer generated heterogeneous materials in other literature. In the real material, cortical bone, the sample surface arising from the exposure of dominant microstructural features was suggested as the source of the observed size effect. In the computer generated material, a two dimensional, closed cell foam, rupturing of cells adjacent to the surface and the associated increase in the compliance of the material located there resulted in a negative size effect being numerically predicted. It has been demonstrated here that these negative effects are entirely in accordance with the behaviour of the simple laminate material.

While negative size effects were reported previously no attempt was made to explain them in the context of generalised continuum theories nor identify any associated constitutive properties, presumably because the nature of the observed effects contradicted the predictions of such theories. Identification of constitutive properties is the central intent of mechanical testing of materials since such property data provide a rational basis for comparing the practical performance of materials when loaded. However, it appears that this intention cannot be fulfilled in the case of a heterogeneous material that displays a negative size effect. Nevertheless, the fact that the negative size effects forecast for both the simple laminated and the more involved perforated materials considered here apparently reflect the positive size effects exhibited when these materials actually behave as generalised continua in the orthodox manner, may offer a pragmatic response to this dilemma since it might be possible to infer constitutive property data from observed effects in the case where they are negative.

Acknowledgements

While undertaking this work Jamie Frame was supported by a PhD studentship funded by the Engineering and Physical Sciences Research Council (EPSRC) – United Kingdom through the Doctoral Training Centre in Medical Devices based at the Department of Biomedical Engineering, University of Strathclyde.

References

Anderson, W.B., Lakes, R.S., 1994. Size effects due to Cosserat elasticity and surface damage in closed-cell polymethacrylimide foam. J. Mater. Sci. 29 (24), 6413–6419.

Bacca, M., Bigoni, D., Dal Corso, F., Veber, D., 2013a. Mindlin second-gradient elastic properties from dilute two-phase Cauchy-elastic composites. Part I: Closed form expression for the effective higher-order constitutive tensor. Int. J. Solids Struct. 50, 4010–4019.

Bacca, M., Bigoni, D., Dal Corso, F., Veber, D., 2013b. Mindlin second-gradient elastic properties from dilute two-phase Cauchy-elastic composites. Part II: Higher-order constitutive properties and application cases. Int. J. Solids Struct. 50, 4020–4029.

Bažant, Z.P., Christensen, M., 1972. Analogy between micropolar continuum and grid frameworks under initial stress. Int. J. Solids Struct. 8, 327–346.

Beveridge, A.J., Wheel, M.A., Nash, D.H., 2013. The micropolar elastic behaviour of model macroscopically heterogeneous materials. Int. J. Solids Struct. 50, 246–255.

Bigoni, D., Drugan, W.J., 2007. Analytical derivation of Cosserat moduli via homogenization of heterogeneous elastic materials. J. Appl. Mech. 74, 741–753.

Choi, K., Kuhn, J.L., Ciarelli, M.J., Goldstein, S.A., 1990. The elastic moduli of human subchondral, trabecular, and cortical bone tissue and the size-dependency of cortical bone modulus. J. Biomech. 23 (11), 1103–1113.

Dai, G.M., Zhang, W.H., 2008. Size effects of basic cell in static analysis of sandwich beams. Int. J. Solids Struct., 2512–2533

Eringen, A.C., 1999. Microcontinuum Field Theories I: Foundations and Solids. Springer-Verlag, New York.

Fleck, N.A., Muller, G.M., Ashby, M.F., Hutchinson, J.W., 1994. Strain gradient plasticity: theory and experiment. Acta Metallur. Mater. 42 (2), 475–487.

Forest, S., Sab, K., 1998. Cosserat overall modeling of heterogeneous materials. Mech. Res. Commun. 25 (4), 449–454.

Gao, X.L., Mahmoud, F.F., 2014. A new Bernoulli–Euler beam model incorporating microstructure and surface energy effects. Zeit. Angew. Math. Phys.(ZAMP) 65, 393–404.

Herrmann, G., Achenbach, J.D., 1968. Applications of theories of generalized Cosserat continua to the dynamics of composite materials. In: Kröner, E. (Ed.), Mechanics of Generalized Continua, Proc. IUTAM Symposium. Springer, Berlin, pp. 69–79.

Lakes, R.S., 1983. Size effects and micromechanics of a porous solid. J. Mater. Sci. 18, 2572–2580.

Lakes, R.S., 1986. Experimental microelasticity of two porous solids. Int. J. Solids Struct. 22, 55–63.

Lakes, R.S., 1995. Experimental methods for study of Cosserat elastic solids and other generalized elastic continua. In: Mühlhaus, H. (Ed.), Continuum Models for Materials with Micro-Structure. Wiley, New York, pp. 1–25.

McGregor, M., Wheel M.A., 2014. On the coupling number and characteristic length of micropolar media of differing topology. In: Proceedings of the Royal Society A, p. 470.

Tekoglu, C., Onck, P.R., 2008. Size effects in two-dimensional Voronoi foams: a comparison between generalized continua and discrete models. J. Mech. Phys. Solids 56, 3541–3564.

Waseem, A., Beveridge, A.J., Wheel, M.A., Nash, D., 2013. The influence of void size on the micropolar constitutive properties of model heterogeneous materials. Eur. J. Mech. A: Solids 40, 148–157.

Yang, J.F.C., Lakes, R.S., 1982. Experimental study of micropolar and couple stress elasticity in bone in bending. J. Biomech. 15, 91–98.